FIBER AMPLIFIERS FOR THIRD GENERATION GRAVITATIONAL WAVE DETECTORS

CEDRIC WILLIAMS[1, 2]

[1]*Department of Physics and Astronomy, Louisiana State University, Baton Rouge, 70803, USA*

[2]*Laser Zentrum Hannover e. V., Hollerithallee 8, 30419, Hannover, Germany*

The future of gravitational wave detection lies in laser and optical technological advances, and in the scientific art of noise control. A likely candidate for third generational interferometer laser signal amplification is the Erbium Doped Fiber Amplifier (EDFA); however, Erbium ions have significant absorption at wavelengths not available from high-power high-brightness pump diodes. As such, EDFA arrangements require alternative pump sources. Taking into account that gravitational wave detectors experience signal sensitivity dominated by pump modulation in low frequencies, we propose a Raman amalgamation. The following is a report on the investigation of a Cascaded Raman Fiber Laser configuration involving the characterization of its behavior due to pump frequency and power modulation. This investigation occurred at the Laser Zentrum Hannover (LZH) in Hannover, Germany as a part of the International Research Experience for Undergraduates (IREU), a program directed by the University of Florida.

I. Introduction

Electromagnetic Radiation has served as mankind's primary tool for observing the universe since the first men gazed upon the stars and sands around them. Even after we met the limitations of our own eyes, we were able to join the ranks of various other species on our planet in the observation of electromagnetic radiation outside of visible light. Where we couldn't look before, infrared and ultraviolet radiation has shown us a way; we haven't looked back since.

Yet, we wish to widen our observable horizons still. Since the advent of Einstein's Special Theory of Relativity and its prediction of the existence of gravitational waves, the idea that we may one day be able to observe the universe in a way not available to us before is capturing the imaginations of people around the world. As of right now, this idea coming to fruition rests on the direct detection of gravitational radiation.

II. First Generation of Gravitational Wave Interferometers

At the forefront of gravitational wave detection is laser interferometry. Projects like the Laser Interferometer Gravitational-Wave Observatory (LIGO) **[Fig. 1a]**, the Virgo gravitational wave observatory **[Fig. 2a]**, and the GEO600 **[Fig. 3a]** have been trying to detect a gravitational wave signal for the past decade, though none have been detected just yet. Nonetheless, great progress has been made in interferometer design. Thanks to the measurements taken by these projects, we have a great and ever-growing understanding of strain sensitivity, a quantitative look at the noise experienced by laser interferometers and the causes thereof. **[see Figures 1b, 2b, and 3b]**. The LIGO and Virgo detectors got close to their design sensitivities, and were able to maintain these sensitivities for long periods of time. LIGO and Virgo have been able to achieve duty cycles of around 80%, while GEO600 managed to stay in science mode 86% of the time between November 2007 and June 2009. This first generation of interferometers also provides us with the necessary infrastructure to support the second generation of detectors. **[6]**

Fig. 1a. LIGO site at Livingston, LA (top) and at Hanford, WA (bottom). [1]

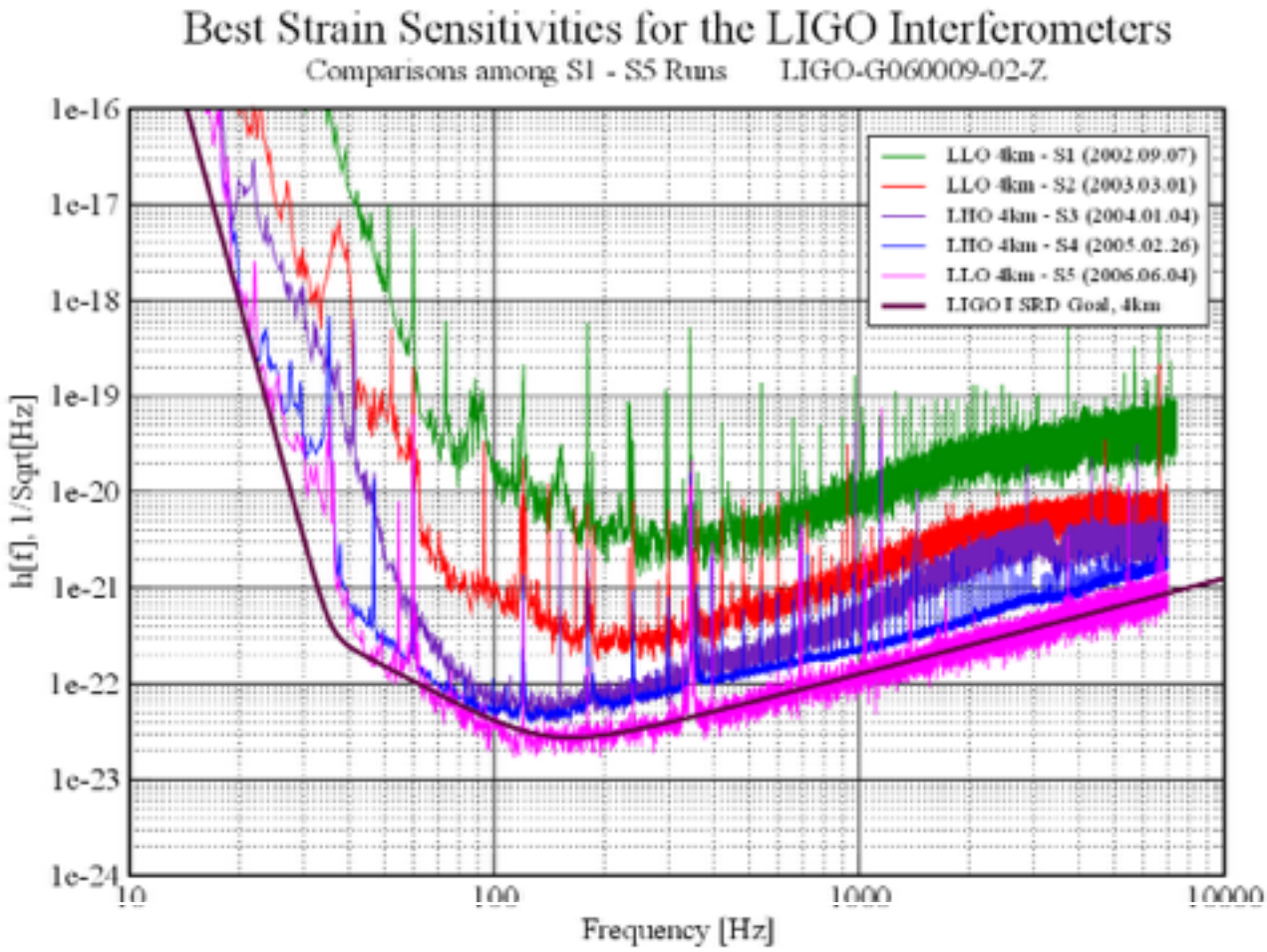

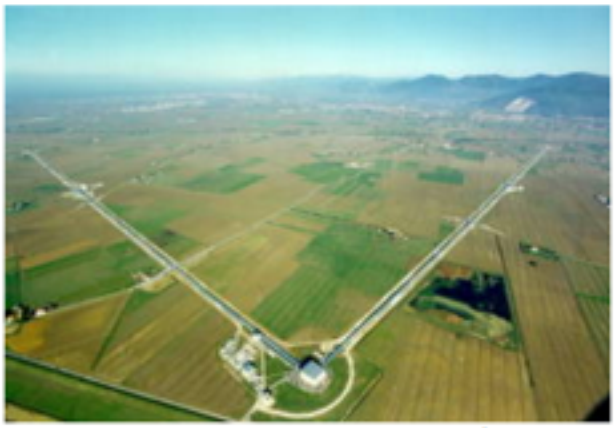

© Eurelios 2000

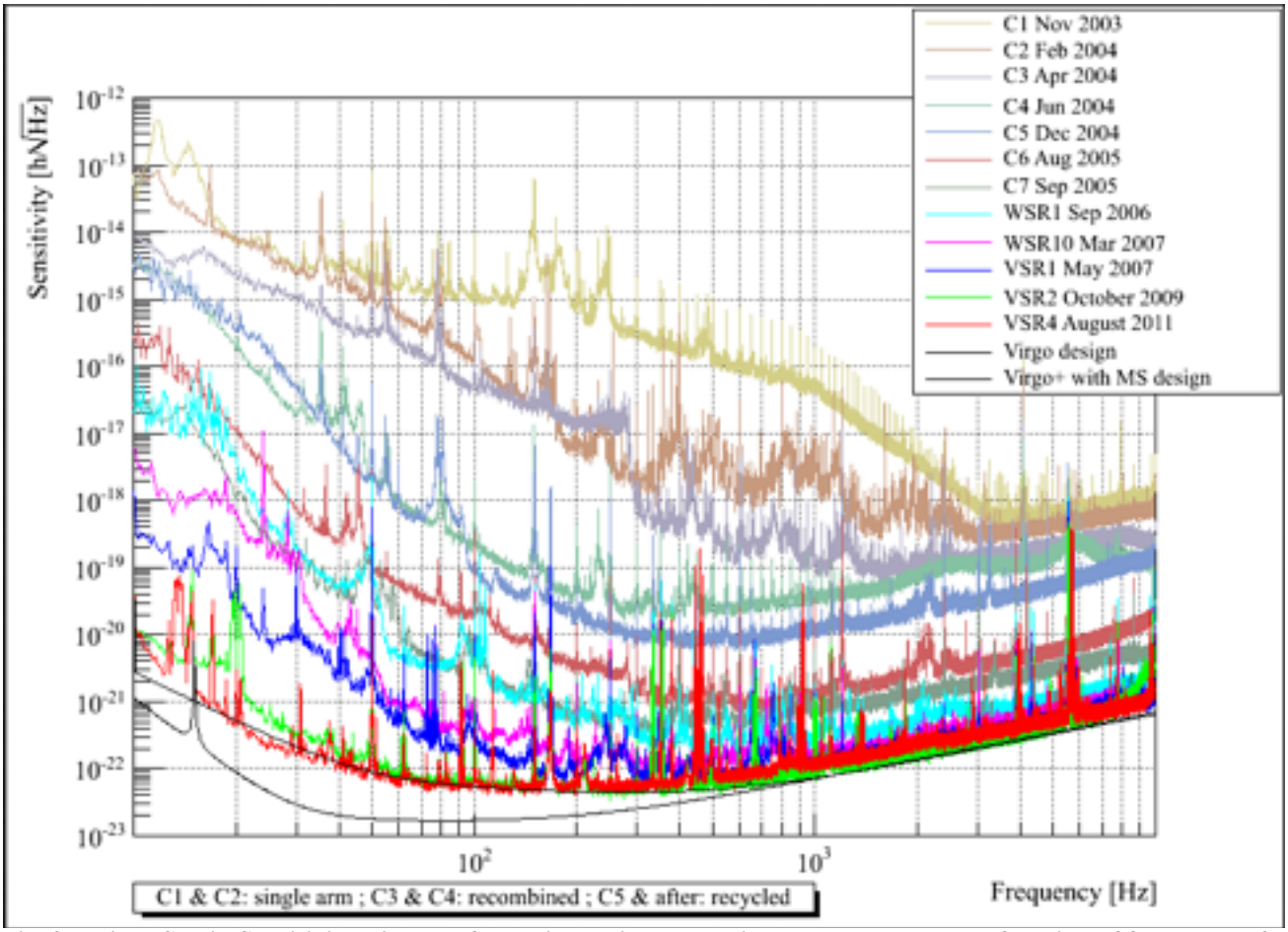

Fig. 2b. Virgo Strain Sensitivity Diagram for various science runs in the past decade as a function of frequency. [3].

Fig. 3a. GEO600 gravitational wave observatory in Hannover, Germany. [4]

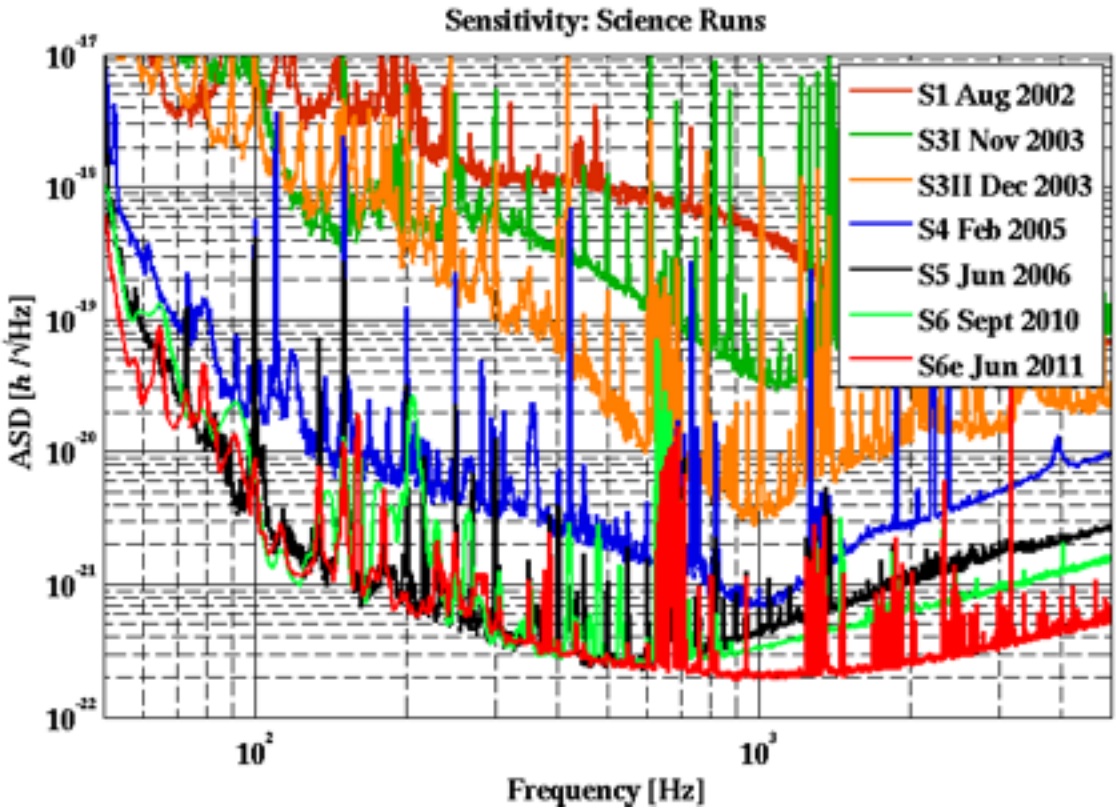

Fig. 3b. GEO600 Strain Sensitivity Diagram for various science runs in the past decade as a function of frequency. [5].

III. Second Generation of Gravitational Wave Interferometers

The upcoming generation of gravitational wave detectors will include upgrades from LIGO to Advanced LIGO (aLIGO) **[7]**, and from Virgo to Advanced Virgo **[8]** (sometimes referred to as AdV). Optimistic assumptions about aLIGO lead to predictions of between 1 and 1000 detections per year upon completion **[9]**. Upgrades include: changes in laser mirror construction to compensate for increased radiation pressure from higher powered beams and thermal lensing, changes in attenuation and suspension equipment to suppress gravity gradient (Newtonian) noise caused by direct gravitational coupling of mass density fluctuations to the suspended mirrors, and significant changes in laser design to increase power and detector frequency range **[6] [10]**. These reconfigurations are set to take place over the next 1 to 3 years, with science runs planned for as early as 2015 (aLIGO). As of 26-May, aLIGO (Livingston) has achieved system locking, indicating that the critical subsystems of the interferometer are functioning successfully, are working well together and are ready for the addition of final parts **[11]**. The gravitational wave community is looking to expand as well. A 3 km underground detector has been funded in Japan, the Kamioka Gravitational Wave Detector (KAGRA), whereas of 31-March-2014 excavation has been completed. KAGRA seeks to join the second generation network as early as 2017. A proposal for a LIGO-India has also been put forth. Proposed by the IndIGO Consortium, the detector is designed as a 4 km arm-length Michelson Interferometer with Fabry-Perot enhancement arms, and aims to detect fractional changes in the arm-length smaller than 10^{-23} $Hz^{-1/2}$ **[12]**. Though we are not quite at the point of second generational science runs, there are already plans for the next series of upgrades, and even new detectors, set to take place and be built around the world; technology must keep up for this third generation.

IV. Third Generation of Gravitational Wave Interferometers

With thermal noise due to mirror coatings and quantum noise arising from a combination of shot noise and radiation pressure noise being the major contributors to interferometer limiting noise, third generational detector technologies must advance beyond these limitations in order to achieve significant sensitivity improvements. Advancements in optical and laser technologies will play a major role in improving signal sensitivity.

The next generation of gravitational wave detectors will use Nd:YAG lasers at $\lambda = 1.064\mu m$ with output powers of up to 200W. The 3rd generation of interferometers will likely incorporate a variety of different laser types, depending on the optical configurations of each site. Some suggest that these detectors might operate with lasers at 1064nm and/or at 1.55µm. Mirror substrate changes are cited as the reason for the use of 1.55µm. Fused silica is the current substrate of choice, but silicon is being considered. Since silicon is not transparent at 1µm, but at 1.55µm, the laser wavelength will have to be adapted. **[13]** EDFAs are prime candidates for producing coherent light at this wavelength, but Erbium experiences good absorption with pump lasers at 1480 nm. There are no diodes available at this wavelength; therefore, alternative pumping methods must be used. This is the motivation at the LZH for working with a cascaded Raman fiber laser. Such 1480 nm configurations have been demonstrated at 67 W and 104 W, which indicate a possibility of success; all that remains is a characterization of the system with regards to the modulating of pump powers and laser signal source frequency. **[14][15]** This is the purpose of this project. The following sections detail my study of the cascaded Raman fiber laser configuration.

V. Mathematical Formalism

In terms of classical analysis, SRS is formalized as a system of 2n+1 first order time dependent coupled differential equations **[16]** :

, (1)

with P_0 indicating pump power, and $P_i^{\pm}$ indicating the power of the i-th Stokes order (i = 1, 2, ..., n). The + and – superscripts indicate forward or backward propagations respectively, while c_0 and c_i indicate pump and i-th Stokes order wave propagation speeds within the fiber. Represented by ν_i is the frequency of the i-th Stokes order, with ν_0 being that of the pump; g_i is the Raman gain coefficient which is related to the cross section of Spontaneous Raman scattering (further discussed below) while α_i accounts for fiber losses at the i-th frequency. The parameter

(2)

represents the spontaneous Raman effect, where h is the Planck constant, ν_i retains its previous definition, and $B_{eff,i}$ is the effective bandwidth for the i-th Stokes order, given by the bandwidth of the corresponding fiber Bragg gratings. β_i depends on the phonon occupancy

(3)

where k_b is the Boltzmann constant, T the temperature, and $\Delta\nu$ the Raman frequency shift (13.2 THz for silica fibers). Given the Raman gain g_α at some wavelength λ_α, the Raman gain coefficient for the i-th Stokes order, at wavelength λ_i, is calculated using

. (4)

The effective interaction area

(5)

between the i - 1 and i Stokes orders is related to the mode field radius

(6)

of each Stokes order involved, and may thus be calculated, given the core radius a and the V number of the fiber.
The initial pump power at z = 0 and the fiber Bragg gratings for the Stokes orders impose additional boundary conditions

(7)

with $R_{left,i}$ and $R_{right,i}$ being the reflectivity of the left and right fiber Bragg grating of the i-th Stokes order. Equations **(1)** and **(7)** constitute a time dependent boundary value problem (BVP), which cannot be solved analytically. Several numerical methods have been used to solve BVPs with vanishing time derivatives **[17][19]**, including the FORTRAN shooting-method solver BVP_SOLVER **[18][20]**. With the aim of obtaining the transfer functions of our cascaded Raman fiber lasers, it is useful to consider a sinusoidal modulation of input pump power

(8)

with a small modulation depth, δ, to account for nonlinearities. Using in Eq. **(1)** a corresponding Ansatz for the pump power and the power of the Stokes orders

(9)

where superscripted 0 indicates the steady state solution yields

, (10)

.

Since these equations are linear in p_0 and p_i, the Fourier Transformations

, (11)

are also a solution, thus obtaining

, (12)

.

with boundary conditions

, (13)

, .

Equations **(12)** and **(13)** now constitute an n+1-dimensional complex BVP. Given the steady state solutions, the transfer functions of the cascaded Raman fiber laser may be calculated by comparing the input and output magnitudes and phases of the complex solutions as demonstrated in **[21]**. The following sections discuss the experimental procedure for measuring said transfer functions.

VI. Experimental Procedure

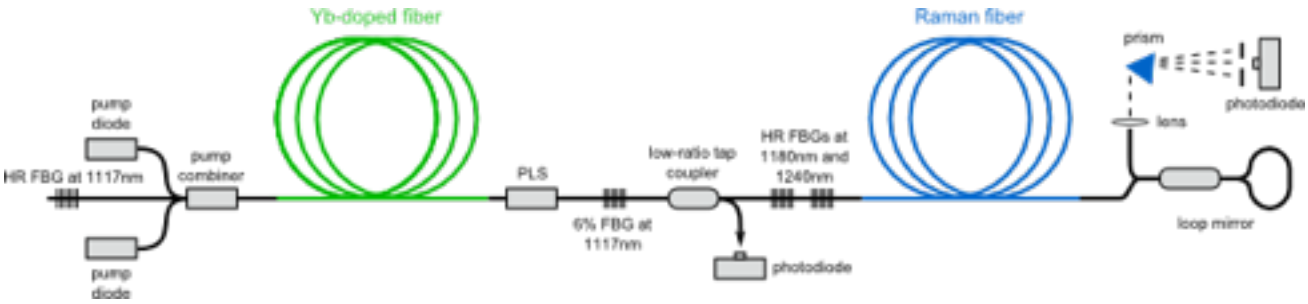

Fig. 4. Set up of the cascaded Raman fiber laser, courtesy of Michael Steinke at Laser Zentrum Hannover. HR FBG high reflectivity FBG.

doped fiber laser source serves as the initial seed source, followed by a Raman resonator consisting of nested fiber Bragg grating (FBG) pairs and a small effective area fiber providing the Raman gain. The FBGs and initial pump power set the boundary conditions of Equation **(13)**. In order to probe the incoming seed for the Raman gain stage, a low-ratio tap coupler was placed after the 6 % FBG at 1117 nm. Naturally a photodiode was placed at the output of the configuration in order to probe the laser light produced. Before we could proceed with our analysis, adjustments had to be made to better suit the oscillating current source for the initial photo diodes. This involved the design and creation of a current buffer. For good measure, I provide a typical transfer curve **[Fig. 5]** from input signal to output signal over the buffer. The buffer was designed to exhibit low pass behavior with a cutoff frequency at around 10 MHz.

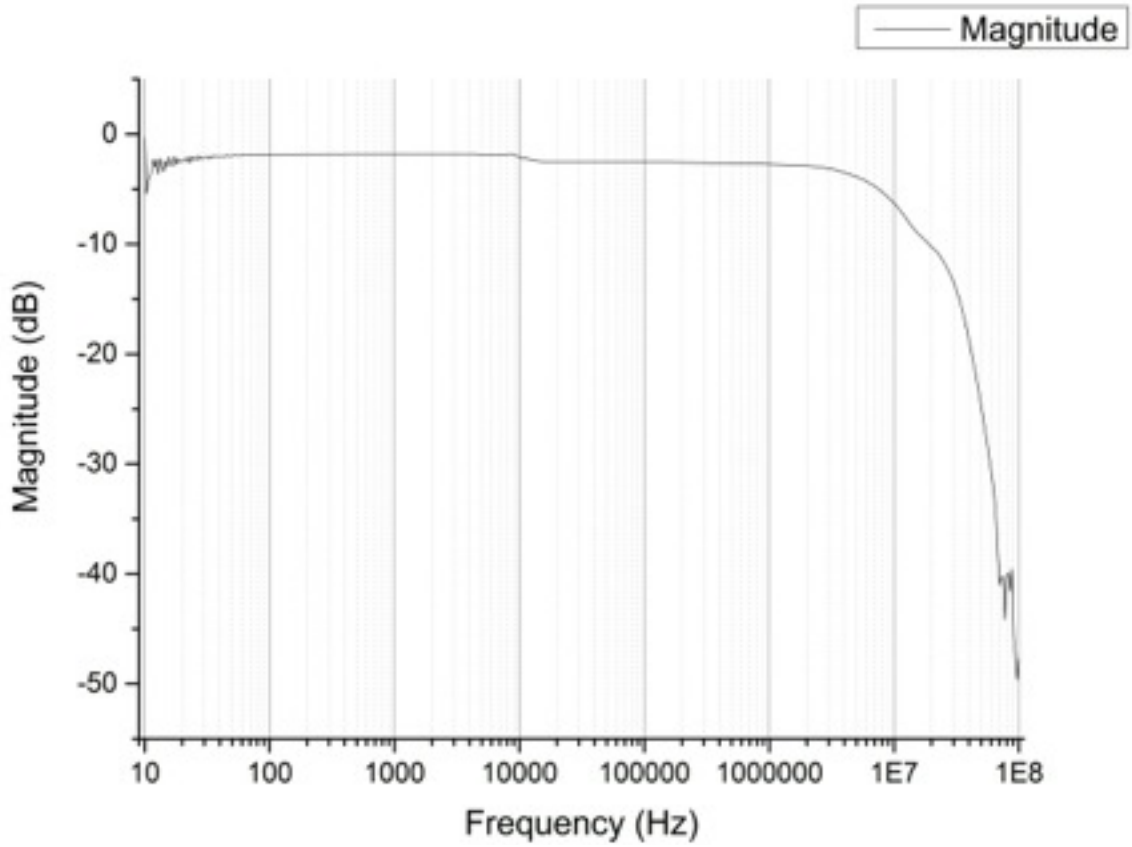

Fig. 5 Typical transfer function curve for current buffer.

first order Stokes signal with residual pump power. The configuration's response to changes in source power also exhibits quite predictable behaviour. The gaps between the transfer curves closer to 0 dB and the lower 4 indicate the suppression of the residual pump and 1st order Stokes signals as the 2nd order Stokes signal begins to lase. At these power levels, predictably, the transfer curves begin to shift from low pass behaviour. The suppression and power levels are further discussed in the next section.

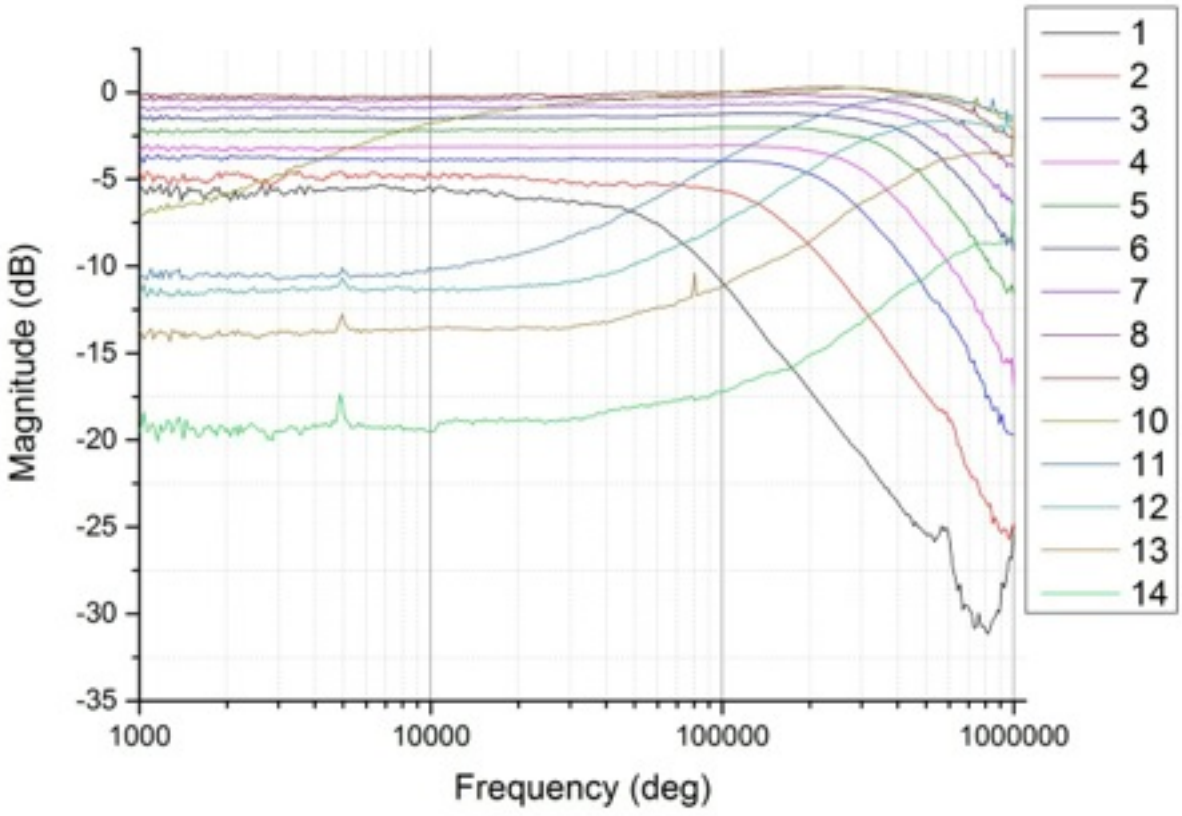

Fig. 6 Laser transfer function over various initial seed powers.

VII. Characterization

In order to further understand the Raman configuration's response to changes in power, we collected output power data. **[Fig. 7]**. The plot indicates a suppression of the 1180 nm light, the 1st order Stokes wave, as soon as the power threshold for the 1240 nm light, the 2nd order Stokes wave, is met. This is to be expected. Limitations on time and unexpected complications with measuring instruments prevented us from continuing this analysis or collecting a larger volume of data points, but this plot is expected to follow theoretical model predictions as more Stokes orders begin to lase. **[Fig. 8]**. Finally, I provide optical spectra plots over various pump powers (represented by increasing currents) for our in lab model **[Fig. 9]**. Encouragingly, the plots show distinct peaks at around 1117 nm, 1180 nm, and 1240 nm, the residual pump, 1st order Stokes signal, and 2nd order Stokes signal wavelengths respectively.

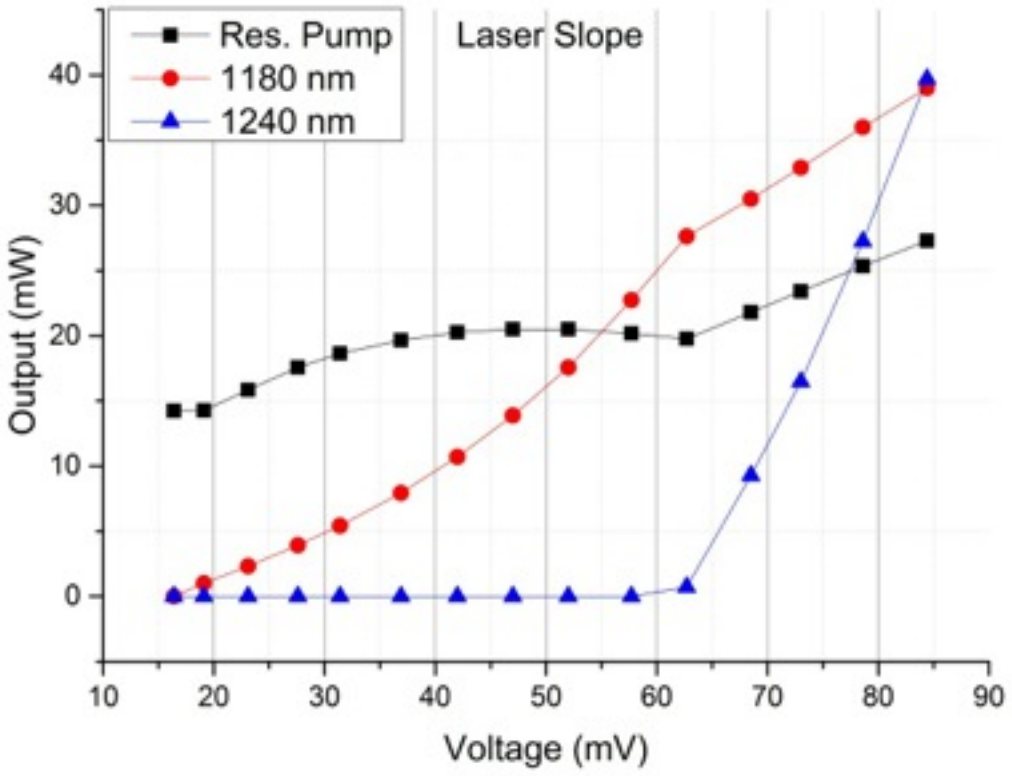

Fig. 7 Plot of total output power of the laser vs. input signal voltage.

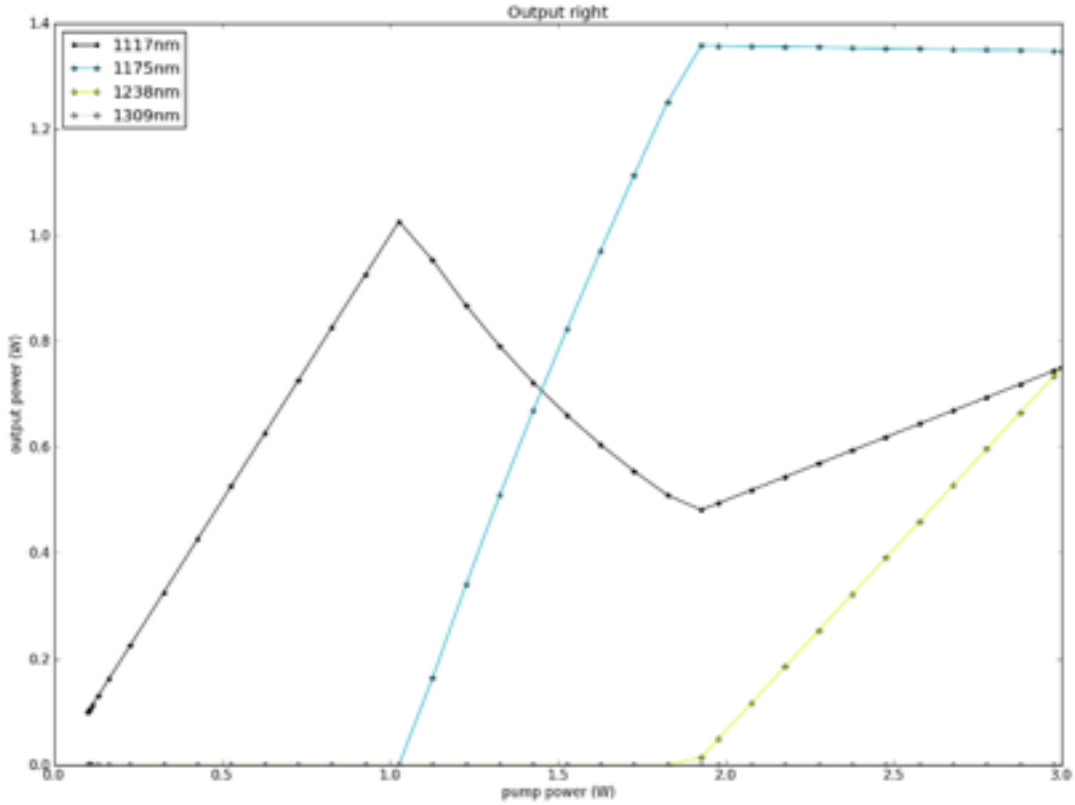

Fig. 8 Theoretical modal plot of total output power of the laser vs. input signal voltage.

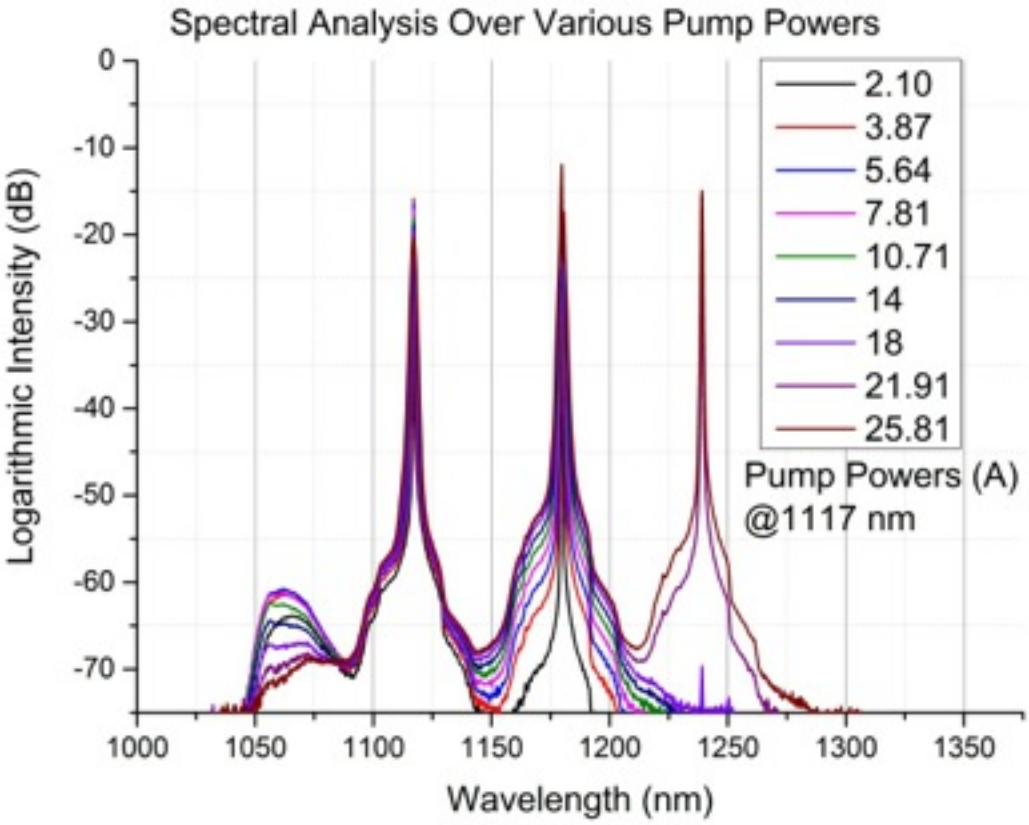

Fig. 9 Optical Spectra over various pump powers. The curves are denoted by a measure of the pump current in Amperes.

A

This project was funded by the Howard Hughes Medical Institute, in collaboration with the National Science Foundation funded International Research Experience for Undergraduates (IREU) at the University of Florida. I would like to thank Dr. Jennifer Loftin for directing me to the program and funding, as well as Dr. Bernard Whiting and Dr. Guido Müller for accepting me, and for the lessons in German. I would also like to thank Kristin Nichola for her vital support, without which I would most likely still be lost in the Netherlands.

Ich möchte Dr. Peter Weßels und Michael Steinke danken. Their teachings and guidance will prove to be invaluable. Lastly, I would like to thank the Laser Zentrum for hosting me.

References

1. The LIGO Scientific Collaboration: B. Abbott, et al, "LIGO: The Laser Interferometer Gravitational-Wave Observatory," Rept.Prog.Phys.72:076901, (2009).

2. J. Zweizig, A. Lazzarini, LIGO Document Control Center. This image can be found at https://dcc.ligo.org/LIGO-G060009/public.

3. These images can be found at https://wwwcascina.virgo.infn.it, courtesy of the Virgo collaboration.

4. This image can be found at http://www.gac-grid.de/project-products/Applications/Geo600.html, courtesy of the German Astronomy Community Grid (GACG).

5. This image can be found at http://www.geo600.org/1032083/GEO600_Sensitivity_Curves, courtesy of the GEO600 gravitational wave detector collaboration.

6. G. Losurdo, “Ground-based gravitational wave interferometric detectors of the first and second generation: an overview,” Class. Quantum Grav. 29 124005 (2012).

7. G. M. Harry, for the LIGO Scientific Collaboration. “Advanced LIGO: the next generation of gravitational wave detectors,” Class. Quantum Grav. 27 084006 (2010).

8. The Virgo Collaboration: T. Accadia, et al, “Status of the Virgo Project,” Class. Quantum Grav. 28 114002 (2011)

9. The LIGO Scientific Collaboration and the Virgo Scientific Collaboration: J. Abadie, et al, “Predictions for the rates of compact binary coalescences observable by ground-based gravitational-wave detectors,” Class. Quantum Grav. 27 173001 (2010).

10. M. Pitkin, S. Reid, S. Rowan, J. Hough, "Gravitational Wave Detection by Interferometry (Ground and Space)" Living Rev. Relativity 14, (2011).

11. D. Shoemaker, “Livingston Locks Advanced LIGO Detector,” Advanced LIGO MIT website (2014).

12. B. Iyer, T. Souradeep, et al (Indian Initiative in Gravitational Wave Observations), “LIGO-India: Proposal for an Interferometric Gravitational-Wave Observatory” (2011).

13. N. Mavalvala, D. E. McClelland, G. Mueller, et al, “Lasers and optics: looking towards third generation gravitational wave detectors” General Relativity and Gravitation (2010) DOI 10.1007/s10714-010-1023-3

14. J. W. Nicholson, “High-power, continuous wave, erbium-doped fiber laser pumped by a 1480 nm Raman fiber laser.” Proc. SPIE 8237, Fiber Lasers IX: Technology, Systems, and Applications, 82370K (23 February 2012); doi: 10.1117/12.908234

15. V. R. Supradeepa, J. W. Nichsolson, et al, “Cascaded Raman Fiber Laser at 1480 nm with Output Power of 104W,” Fiber Lasers IX: Technology, Systems, and Applications, 82370J (2012) doi: 10.1117/12.908539

16. G. P. Agrawal, *Nonlinear Fiber Optics*, 4th ed (Academic, 2007)

17. S. D. Jackson, and P. H. Muir, “Theory and numerical simulation of n-th order cascaded Raman fiber lasers,” J. Opt. Soc. Am. B 18, 1297-1306 (2001)

18. L. F. Shampine, P. H. Muir and H. Xu, “A User-Friendly Fortran BVP Solver,” Journal of Numerical Analysis, Industrial and Applied Mathematics 1, 201-217 (2006)

19. J. Salvatier, “scikits.byp_solver 1.1,” https://pypi.python.org/pypi/scikits.bvp_solver

20. M. Steinke, E. Schreiber, D. Kracht, J. Neumann, and P. Wessels, “Development of a cascaded Raman fiber laser with 6.5 W output power at 1480 nm supported by detailed numerical simulations,” in 2013 Conference on Lasers and Electro-Optics – International Quantum Electronics Conference, (Optical Society of America, 2013), paper CJ-P.16

21. M. Krause, S. Cierullies, H. Renner, and E. Brinkmeyer, “Pump-to-Stokes RIN transfer in Raman fiber lasers and its impact on the performance of co-pumped Raman amplifiers,” Opt. Commun. 260, 656-661 (2006)